Optimization of adeno-associated virus (AAV) gene delivery into human bone marrow stem cells (hBMSCs)

Shaomian Yao[1], Weiqiong Rong[1], Yuanying Yuan[1], and Xue Wen[1]

[1]Louisiana State University System

July 8, 2022

Abstract

Efficiently delivering nucleic acid into mammalian cells is essential to overexpress genes for assessing gene functions. Human bone marrow stem cells (hBMSCs) are the most studied tissue-derived stem cells. Adeno-associated viruses (AAVs) have been used to deliver DNA into hBMSCs for various purposes. This study optimized the AAV transduction protocol for high-efficiency DNA delivery into hBMSCs. hBMSCs were infected with different serotypes of AAVs containing green fluorescence (eGFP) reporter driven by the CMV promoter. GFP was monitored in the infected cells. Cells were collected at designated time points after the infection for RT-PCR to assess eGFP mRNA. The results indicated that the order of transduction efficiency of the AAV serotypes was AAV2 > AAV2.7 > AAV6 > AAV6.2 > AAV1 > AAD-DJ. AAV2 could achieve almost 100% transduction at the MOI greater than 100K. Over 90% of cells could be transduced at 20K to 50K MOI. About 80% transduction was seen at MOIs of 10K and 15K. The eGFP expression reached the maximum about15- 25 days post-AAV2 infection. High levels of transcription were still detectable at day 30 post-infection. We conclude that AAV2 and AAV2.7 can efficiently deliver transgene into hBMSCs for sustained expression over one month.

1. INTRODUCTION

Efficient nucleic acid delivery systems are vital for studying gene function and performing gene therapies. Physical, chemical and biological-based methods are commonly used to deliver genes into mammalian cells. Physical methods (electroporation, sonoporation, microinjection and biolistics or bombardment, etc.) use physical forces to create temporary membrane pores to allow entry of the nucleic acid into cells.[1] However, such methods require expensive equipment and often are inconvenient for most gene delivery applications.[2] More importantly, physical gene delivery generally exhibits lower cell viability due to heavy trauma and apoptotic or programmed cell death caused or induced by the physical forces, thus having limited applications.[3]Chemical methods use natural or synthetic compounds, namely transfection reagents, as nucleic acid carrier molecules to facilitate nucleic acid delivery into cells. Transfection reagents are classified into four major types: calcium phosphate, DEAE-dextran, cationic lipid, and cationic polymer, and each has advantages and disadvantages.[4, 5] Cell toxicity and low transfection efficiency for large DNA (plasmids) are the main disadvantages. Biological methods rely on the infectious property of bacteria or viruses to transfer genes into cells. Viral gene delivery is the most studied method for delivering transgenes into animal cells. If appropriately optimized, it can be the most efficient gene delivery method. Adenoviruses, retroviruses, lentiviruses, and adeno-associated viruses (AAVs) have been used to transfer genes *in vitro* and*in vivo* . Of them, AAVs are attractive virus-based gene delivery candidates as they are innately nonpathogenic and cause a very mild immune response, unlike adenoviruses and retroviruses, which can cause severe immunogenicity and other problems.[6] So far, 12 AAV serotypes (variants within each serotype) have been identified with variable tissue and cell type tropism. It is critical to test different AAVs to achieve optimal gene delivery for various cells and tissues.

Mesenchymal stem cells (MSCs) are adult stem cells primarily residing in the bone marrow. Human

bone marrow mesenchymal stem cells (hBMSCs) possess the multipotent capability to differentiate into osteoblasts, adipocytes, chondrocytes, etc.[7] and are the most frequently used stem cells in cell therapy and tissue engineering.[8] Directing hBMSC differentiation toward desired cell types is vital for the applications of the cells in tissue engineering and regenerative medicine. However, the molecular pathways regulating their differentiation are not fully understood. Developing highly efficient gene delivery methods is essential for molecular biology experiments to elucidate the genes controlling hBMSC differentiation for cell- and gene-based therapies. In this regard, gene delivery into hBMSCs using AAV vectors has been attempted. Ju et al and Ito et al. first reported hBMSC transduction with AAV.[9,10] However, subsequent studies in different laboratories reported inconsistent transduction efficiency of AAVs for hBMSCs showing a high variation of transduction for AAV vectors in human MSCs.[11] The source of variation in AAV vector transduction is currently unknown, likely due to multiple factors, such as, cell culture condition, vector preparation, and transduction conditions.[11] A publication indicated that AAV transduction efficiencies could achieve up to 65%.[12] Thus, further improving AAV transduction is desired. The objectives of this study were to further optimize the AAV transduction and attempt to establish a highly efficient AAV gene delivery system for the *in vitro* transduction of hBMSCs. Additionally, it is our goal to study the longevity of transgene expression in hBMSCs after AAV transduction.

2. MATERIALS AND METHODS

2.1 Culture of human bone marrow stem cells (hBMSCs)

Primary hBMSCs (Passage 0) isolated from two donors which are termed hBMSCs-1 and hBMSCs-2 in this study, were purchased from Obatala Sciences (New Orleans, LA, USA). Purchasing and using human stem cells for research have been approved by the IRB Office of the Louisiana State University. The cells were cultured in T-75 flasks with a medium consisting of MEM-α (Corning) plus 20% FBS (Neuromics) and 1% Penicillin-Streptomycin (Gibco) in 5% CO_2 at 37°C. The culture medium was changed every four days. Cells were passaged at 80-90% confluence at a 1:3 ratio, and different passages were obtained and cryopreserved in liquid N2. Passages 4 and 5 cells were used for the experiments.

2.2 AAVs and transduction experiments

AAVs containing enhanced green fluorescent protein (eGFP) under transcriptional control by a CMV promoter (i.e., AAVs-eGFP) were purchased from VectorBuilder (Chicago, IL, USA). The AAV titers provided by the manufacturer were based on qPCR assessment. The titer of the AAV stocks was adjusted to 10^{12} GC/ml with PBS buffer supplemented with 200 mM NaCl and 0.00067% pluronic F-127. For assessment of transduction efficiency, hBMSCs were seeded in 24-well plates with cell growth medium (MEM-α plus 20% FBS and 1% Penicillin-Streptomycin) in 5% CO_2 at 37°C. When the cells grew to about 90% confluency, AAVs-eGFP were added to 200 μl of the medium (MEM-α plus 20% FBS) in each well with the designated multiplicity of infection (MOI) for infection. The infection medium was replaced with a fresh cell growth medium (0.5 ml/well) after overnight incubation, and the cells were cultured at normal cell culture conditions. To assess the mRNA level of the eGFP, we seeded cells in 12-well plates for AAV2-eGFP infection as described above with 0.5 ml medium/well. Infected cells were cultured in cell growth medium (1 ml/well) with four days of medium change interval and collected at designated time points for RNA extraction.

2.3 Assessment of transduction efficiency

Hoechst 33324 was used to stain the cell nuclei to facilitate counting the cell numbers. Briefly, cells were stained with Hoechst 33324 (5 μg/ml) in cell growth medium for 5 min on days 5, 10, and 15 post-infections. The staining medium was removed, and the cells were washed once with a fresh cell growth medium (0.5 ml/well) to remove the Hoechst dye residual. Three distinct microscopic fields were visualized and photographed first for blue-fluorescent nuclei and then the green-fluorescent image of the same view using a ZOE^{TM}Fluorescent Cell Imager (Bio-Rad). The images were analyzed with ImageJ to acquire total cell numbers by counting blue-fluorescent nuclei. The blue-fluorescent images were merged with the corresponding green-fluorescent images, and green-fluorescent cells (i.e., eGFP-positive cells) were counted twice manually to ensure accuracy. Transduction efficiency was expressed by the percentage of green-fluorescent

cells over the total cells.

2.4 Assessment of longevity of eGFP mRNA expression post-AAV infection

hBMSCs were seeded in 12-well plates and incubated with 20K MOI of AAV2-eGFP. Cells were collected in TRI reagent (Molecular Research Center, Cincinnati, OH, USA) on days 5, 10 15, 20, 25, and 30 post-infections. Total RNA was extracted using the traditional Trizol method (Molecular Research Center, Inc., Cincinnati, OH). Extracted RNA was digested with Turbo^{TM} DNase (ThermoFisher Scientific) to remove possible DNA contamination followed by quantitation by NanoDrop^{TM} 8000 Spectrophotometer (ThermoFisher Scientific). The RNA quality was assessed by OD260/280 and OD260/230. 700-900 ng total RNA was reverse transcribed to 20 µl cDNA with random primers and M-MLV reverse transcriptase (ThermoFisher Scientific), followed by 25 cycles of PCR with 1 µl cDNA to detect eGFP mRNA expression. The primers used for the PCR were as follows: eGFP: CACATGAAGCAGCACGACTTC (forward), GACTGGGTGCTCAGGTAGTG (reverse); Beta-Actin: CCACCATGTACCCTGGCATT (forward); TGTGCAATCAAAGTCCTCGG (reverse). The PCR product was loaded to 1.5% agarose gel containing ethidium bromide for electrophoresis, followed by gel imaging with Bio-Rad ChemiDoc + gel imaging system.

2.5 Statistical analysis

Statistical analysis was performed with the Wilcoxon rank-sum test. The p-values less than 0.05 (*) and 0.01 (**) indicate that the differences between means are statistically significant or highly statistical significance, respectively. Data were presented as mean ± standard deviation (SD).

3. RESULTS

Weak green fluorescence started to appear as early as three days post-infection for AAV2 AAV2.7, AAV6, and AAV6.2 in hBMSCs-1 and hBMSCs-2. And the green fluorescence became bright on day 5 post-infection in some cells, especially for AAV2 and AAV2.7 at the high MOI treatments (Fig. 1). No green fluorescence could be observed in cells infected with AAV1 and AAV-DJ on day 5 (Fig. 1). Only few eGFP-positive cells were seen in AAV1, and AAV-DJ infected cells on days 10 and 15 post-infection (Figs. 2 and 3). AAV1 treatment showed slightly more eGFP-positive cells than AAV-DJ treatment on days 10 and 15 post-infection (Figs. 2 and 3) in both cell lines. The results indicated that AAV1 and AAV-DJ were very inefficient for the transduction of hBMSCs. Thus, AAV1 and AAV-DJ were excluded for further analyses and optimization for hBMSCs transduction. eGFP-positive cells were significantly increased for other serotypes on days 10 and 15. We counted total cells and green-fluorescent cells and calculated the percentage of eGFP-positive cells. The results are shown in Figs. 4-7.

For AAV2 infected cells, more eGFP-positive cells could be seen in hBMSCs-1 than in hBMSCs-2 at 20K and 50K MOI on days 10 and 15 (Fig. 4). For example, more than 90% of the AAV2 treated cells were eGFP positive in hBMSCs-1, but less than 40% of cells were eGFP positive in hBMSCs-2 at 20K MOI on day 10 post-infection. The difference was highly statistically significant ($p < 0.01$). However, at MOI of 100K and 200K, almost all cells in hBMSCs-1 and hBMSCs-2 exhibited eGFP positive (Fig. 4), and there was no significant difference. AAV2.7 showed a similar trend as AAV2 (Fig. 5). At MOI of 20K, very few eGFP-positive cells were seen in hBMSCs-2, whereas most of the cells in hBMSCs-1 were eGFP positive. However, when MOI was greater than 100K, most cells ($> 80\%$) in both hBMSCs-1 and hBMSCs-2 were eGFP positive, although hBMSCs-1 still had higher transduction efficiency than hBMSCs-2.

MOIs and the genetic background of the hBMSCs appeared to have a huge impact on transduction efficiency for AAV6 and AAV6.2. Very few eGFP-positive cells (less than 10%) were seen in the treatments of MOIs 20K and 50K. Significant increases of eGFP-positive cells were observed as MOI increased to 100K and 200K. Approximately 80-90% cells were eGFP positive for hBMSCs-1, and 40% cells were eGFP positive for hBMSCs-2 on day 15 post-infection. The differences in the percentage of eGFP-positive cells between hBMSCs-1 and hBMSCs-2 were statistically significant (Figs. 6 and 7).

The above results made it clear that AAV2 and AAV2.7 were superior to other AAV serotypes for the transduction of hBMSCs. The transduction efficiency of AAV2 and AAV2.7 was less affected by the MOIs,

and cell donors compared to AAV6 and AAV6.2. Since it is desired to use as low as possible MOI of AAVs to infect cells for gene delivery, we reasoned it is possible to further reduce the MOI of AAV2 and AAV2.7. Therefore, we tested AAV2 and AAV2.7 at reduced MOIs of 5K, 10K and 15K for infection of hBMSCs-1. The results are presented in Figs. 8 and 9. Greater than 80% of cells could be transduced at MOIs of 10K, and 15K in AAV2 infected cells on day 15 of post-infection (Fig. 8). AAV2.7 also achieved about 80% transduction with MOI of 15K on day 15 on average (Fig. 9).

The longevity of transgene expression is a critical parameter for assessing gene delivery systems in gene therapy and gene functional study. Thus, we collected AAV2-eGFP infected hBMSCs at different time points for RT-PCR analysis. RT-PCR indicated that the transcription (mRNA) of the transgene (eGFP) could be detected on day 5 post-infection. However, for hBMSCs-1, the expression appeared to reach a maximum around day 15 post-infection, and for hBMSCs-2, maximal expression appeared around day 25 (Fig. 10). It is worth noting that high eGFP mRNA levels were still seen on day 30 post-infection for both cell lines (Fig. 10).

4. DISCUSSION

AAV vectors have been extensively studied for their therapeutic applications and biomedical research. The molecular mechanism of AAV infection and cell entry is still largely unknown.[13] There are many serotypes and variants of AAVs, and different AAV serotypes display significant differences in transduction efficiency and cell and tissue tropism.[14, 15] The selection of appropriate AAV serotypes is among the first things that need to do in designing AAV gene delivery. Here, we tested commonly used serotypes for delivering the eGFP reporter gene into hBMSCs derived from different donors. Our data indicate that serotypes are the most critical factor. Based on our observation, we rank the superiority of those AAVs for transducing hBMSCs as follows regardless of cell donor background: AAV2 > AAV2.7 > AAV6 > AAV6.2 > AAV1 > AAV-DJ.

Using AAVs to deliver transgenes into human MSCs has been attempted, and published data regarding the AAV vector transduction efficiency of stem cells are inconsistent.[11] An early study compared AAV serotypes 1, 2, 3, 4, 5, 6, and 8 to infect MSCs of human and non-human primates and found that AAV2 was the most efficient serotype for human and baboon MSCs.[16] Another study reported that up to 65% transduction could be achieved with AAV2 in human MSCs at 4 days post-transduction.[12] Our data align with those published results showing that AAV2 is the most efficient serotype for transducing hBMSCs. Our experiments showed AAV2 is highly efficient in transferring genes into hBMSCs. High efficiency of transduction (> 80%) could be achieved by simply adding the viral particles to the cell cultures at MOI as low as 10K. Transduction efficiency could reach almost 100% when hBMSCs were infected with high MOI ([?] 100K) of AAV2 or its variant AAV2.7. However, our results suggested that the donor's genetic background could affect the AAV transducing efficiency, especially at the lower MOIs. We noticed that the hBMSCs derived from different donors had a significant impact on transduction efficiency at a low MOI. hBMSCs derived from the donor 1 seem to result in higher transduction efficiency than the hBMSCs from the donor 2; suggesting that hBMSCs' genetic background may impact the transduction efficiency.

In a recent publication, Bougioukli et al. reported that AAV2 and AAV6 had limited potential for delivering transgenes (eGFP and BMP-2) into hBMSCs.[17] on day 7 post-infection. We observed expression of the transgene (eGFP) on day 5 post-AAV infection; however, the maximal expression was not reached until around days 15-25 post-infection. AAV has a single-stranded DNA (ssDNA) genome (i.e., ssAAV). After entering the cells, the ssDNA must be converted to double-stranded DNA (dsDNA) before the transgene can be transcribed to mRNA. Thus, there is a delay in the onset of transgene expression after AAV infection. The ssDNA to dsDNA conversion is a well-documented, rate-limiting step involving the de novo synthesizing the second strand DNA.[18,19] We observed a dramatic increase of green fluorescence beginning on day 10 post-infection. PCR analysis indicated that the maximum eGFP transcription occurs around days 15-25 post-infection depending on cell lines. The delay of transgene expression is one of the disadvantages or limitations of using AAV vector for gene delivery applications; especially, immediate therapeutic intervention is needed. One approach is to use self-complementary AAVs (scAAVs), which circumvent second-strand DNA synthesis requirements to overcome this limitation. scAAV has been demonstrated to exhibit faster, stronger,

and prolonged transgene expression.[20]However, the cargo capacity of scAAV (5' ITR to 3' ITR) that can be properly packaged into mature viral particles is only about half that of conventional ssAAV.

In summary, our data suggested that AAV1 and AAV-DJ have minimal transduction ability for hBMSCs. Although AAV6 and its variant AAV6.2 can deliver transgenes into hBMSCs, their transduction efficiency is largely affected by MOI. The use of high MOI is needed to result in considerable transduction for AAV6 and AAV6.2. In contrast, AAV2 and its variant AAV2.7 can efficiently deliver transgene into hBMSCs with almost 100% transduction efficiency; however, AAV2 appears superior to AAV2.7. At an MOI less than 50K, hBMSCs derived from different donors may exhibit the discrepancy in transduction efficiency with AAV2. However, at an MOI greater than 100K, AAV2 appears to transduce hBMSCs derived from different donors without significant difference.

ACKNOWLEDGEMENTS

This research was supported by the National Institutes of Health / National Institute of Arthritis and Musculoskeletal and Skin Diseases (1R21AR076583-01A1). Shaomian Yao: Conceptualization, Methodology, Validation, Data analysis and curation, Manuscript draft and revision, Project administration, Funding acquisition. Weiqiong Rong: Experiment preparation, Investigation, and Manuscript review; Yuanying Yuan: Data collection and Manuscript review. Xue Wen: Statistical analysis and Manuscript review.

CONFLICT OF INTEREST

All authors declare no conflict of interest.

Data availability statement: The data that support the findings of this study are available from the corresponding author upon reasonable request.

REFERENCES

1. Mehier-Humbert S, Guy RH. (2005). Physical methods for gene transfer: improving the kinetics of gene delivery into cells. *Adv Drug Deliv Rev.* 57(5):733-753.

2. Bono N, Ponti F, Mantovani D, Candiani G. (2020). Non-Viral in Vitro Gene Delivery: It is Now Time to Set the Bar! *Pharmaceutics.*12(2):183.

3. Mellott AJ, Forrest ML, Detamore MS. (2013). Physical non-viral gene delivery methods for tissue engineering. *Ann Biomed Eng.*41(3):446-468.

4. Gao X, Kim KS, Liu D. (2007). Nonviral gene delivery: what we know and what is next. *AAPS J.* 9(1):E92-104.

5. Fus-Kujawa A, Prus P, Bajdak-Rusinek K, Teper P, Gawron K, Kowalczuk A, Sieron AL. (2021). An Overview of Methods and Tools for Transfection of Eukaryotic Cells in vitro. *Front Bioeng Biotechnol.* 9:701031.

6. Samulski RJ, Muzyczka N. (2014). AAV-Mediated Gene Therapy for Research and Therapeutic Purposes.*Annu Rev Virol.* 1(1):427-451

7. Kassem M, Abdallah BM. (2008). Human bone-marrow-derived mesenchymal stem cells: biological characteristics and potential role in therapy of degenerative diseases. *Cell Tissue Res.* 331(1):157-163.

8. Fu X, Liu G, Halim A, Ju Y, Luo Q, Song AG. (2019). Mesenchymal Stem Cell Migration and Tissue Repair. *Cells* . 8(8):784.

9. Ju XD, Lou SQ, Wang WG, Peng JQ, Tian H. (2004). Effect of hydroxyurea and etoposide on transduction of human bone marrow mesenchymal stem and progenitor cell by adeno-associated virus vectors.*Acta Pharmacol Sin.* 25(2):196-202.

10. Ito H, Goater JJ, Tiyapatanaputi P, Rubery PT, O'Keefe RJ, Schwarz EM. (2004). Light-activated gene transduction of recombinant adeno-associated virus in human mesenchymal stem cells. *Gene Ther.* 11(1):34-41.

11. Brown N, Song L, Kollu NR, Hirsch ML. (2017). Adeno-Associated Virus Vectors and Stem Cells: Friends or Foes? *Hum Gene Ther.*28(6):450-463.

12. Stender S, Murphy M, O'Brien T, Stengaard C, Ulrich-Vinther M, Soballe K, Barry F. (2007). Adeno-associated viral vector transduction of human mesenchymal stem cells. *Eur Cell Mater.* 13:93-99; discussion 99.

13. Berry GE, Asokan A. (2016). Cellular transduction mechanisms of adeno-associated viral vectors. *Curr Opin Virol.* 21:54-60.

14. Wiley LA, Burnight ER, Kaalberg EE, Jiao C, Riker MJ, Halder JA, Luse MA, Han IC, Russell SR, Sohn EH, Stone EM, Tucker BA, Mullins RF. (2018). Assessment of Adeno-Associated Virus Serotype Tropism in Human Retinal Explants. *Hum Gene Ther* . 29(4):424-436.

15. Srivastava A. (2016). In vivo tissue-tropism of adeno-associated viral vectors. Curr Opin Virol. 21:75-80.

16. Chng K, Larsen SR, Zhou S, Wright JF, Martiniello-Wilks R, Rasko JE. (2007). Specific adeno-associated virus serotypes facilitate efficient gene transfer into human and non-human primate mesenchymal stromal cells. *J Gene Med.* 9(1):22-32.

17. Bougioukli S, Chateau M, Morales H, Vakhshori V, Sugiyama O, Oakes D, Longjohn D, Cannon P, Lieberman JR. (2020). Limited potential of AAV-mediated gene therapy in transducing human mesenchymal stem cells for bone repair applications. *Gene Ther.* 28: 729–739.

18. Ferrari FK, Samulski T, Shenk T, Samulski RJ. (1996). Second-strand synthesis is a rate-limiting step for efficient transduction by recombinant adeno-associated virus vectors. *J Virol.*70(5):3227-3234.

19. Fisher KJ, Gao GP, Weitzman MD, DeMatteo R, Burda JF, Wilson JM. (1996). Transduction with recombinant adeno-associated virus for gene therapy is limited by leading-strand synthesis. *J Virol.*70(1):520-532.

20. Wang Z, Ma HI, Li J, Sun L, Zhang J, Xiao X. (2003). Rapid and highly efficient transduction by double-stranded adeno-associated virus vectors in vitro and in vivo. *Gene Ther.* 10(26): 2105-2111.

Figure legends:

Figure 1. Infection of hBMSCs with different AAV serotypes containing eGFP resulted in distinct green fluorescence patterns on day 5 post-infection. The images shown were from hBMSCs-1. Note that green fluorescence was present in cells transduced with AAV2, AAV2.7, AAV6, and AAV6.2, and almost no fluorescence in cells infected by AAV1 and AAV-DJ.

Figure 2. hBMSCs infected by AAV1-eGFP showed low transduction efficiency on days 10 and 15 post-infection. Note that only scattered green fluorescence appeared even at high MOIs of 100-200K.

Figure 3. AAV-DJ-eGFP showed almost no transduction in hBMSCs on days 10 and 15 post-infection. Note very few cells appeared with green fluorescence even at high MOIs of 100-200K.

Figure 4. hBMSCs infected with AAV2-eGFP showed bright green fluorescence on days 10 and 15 post-infection. Note at 20K and 50K MOIs, hBMSCs-1 showed significantly higher transduction efficiency than hBMSCs-2. In contrast, transduction efficiency had no significant difference at MOI of 100K and 200K, where nearly 100% of cells were transduced. ** indicated that the differences were highly statistically significant at $p < 0.01$.

Figure 5. hBMSCs infected with AAV2.7-eGFP showed bright green fluorescence on days 10 and 15 post-infection. Note in general, hBMSCs-1 showed significantly higher transduction efficiency than hBMSCs-2,

especially at 20K and 50K MOIs. At MOIs of 100K and 200K, nearly 100% of hBMSCs-1 were transduced. In contrast, transduction efficiency showed some variations in hBMSCs-2. * and ** indicated that the differences were significant and highly significant at $p < 0.05$ and$p < 0.01$, respectively.

Figure 6. hBMSCs infected with AAV6-eGFP showed bright green fluorescence on days 10 and 15 post-infection at MOIs of 100K and 200K. Note that hBMSCs-1 showed significantly higher transduction efficiency than hBMSCs-2 at most MOIs. Both cell lines had low transduction efficiency ($< 20\%$) with MOIs less than 50K. * and ** indicated that the differences were significant and highly significant at $p < 0.05$ and $p < 0.01$, respectively.

Fig. 7. hBMSCs infected with AAV6.2-eGFP showed bright green fluorescence on days 10 and 15 post-infection at MOIs of 100K and 200K. Note that hBMSCs-1 showed significantly higher transduction efficiency than hBMSCs-2 at most MOIs. Both cell lines had low transduction efficiency ([?] 20%) with MOIs less than 50K. * and ** indicated that the differences were significant and highly significant at $p< 0.05$ and $p < 0.01$, respectively.

Figure 8. Effects of low MOIs of AAV2-eGFP on transduction of hBMSCs-1. (A) Fluorescent images of the hBMSCs infected with 5K, 10K, and 15K MOI of AAV2-eGFP on days 5, 10, and 15 post-infection. (B) % green-fluorescent cells (i.e., % transduced cells) at different treatments and times.

Figure 9. Effects of low MOIs of AAV2.7-eGFP on transduction of hBMSCs-1. (A) Fluorescent images of the hBMSCs infected with 5K, 10K, and 15K MOI of AAV2.7-eGFP on days 5, 10, and 15 post-infection. (B) % green-fluorescent cells (i.e., % transduced cells) at different treatments and times.

Figure 10. Longevity of eGFP expression in AAV2-eGFP transduced hBMSCs as shown by conventional RT-PCR. Note that transgene expression was clearly detected at day 5 post-infection. The maximal expression of the eGFP appeared around day 15 and day 25 post-infection for hBMSCs-1 and hBMSCs-2, respectively. High levels of transgene (eGFP) expression persisted for 30 days post-infection.

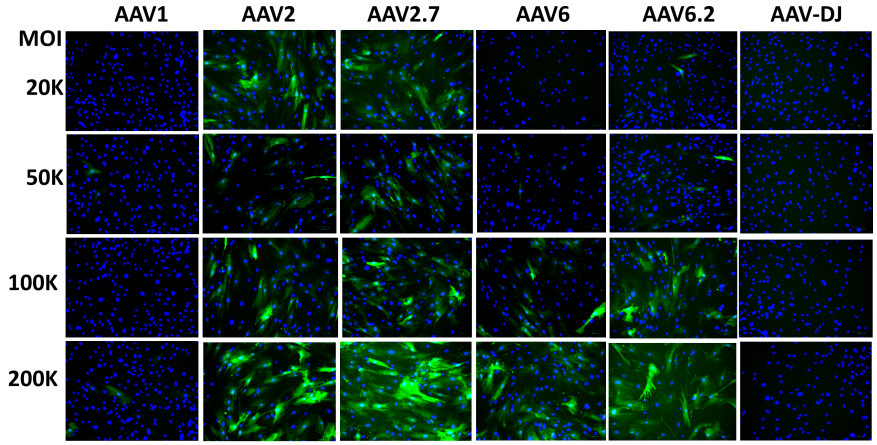

Fig. 1

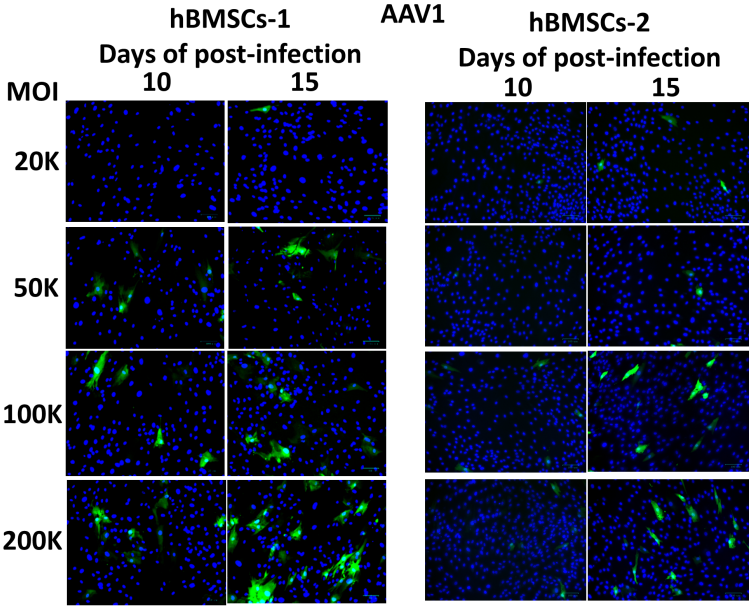

Fig. 2

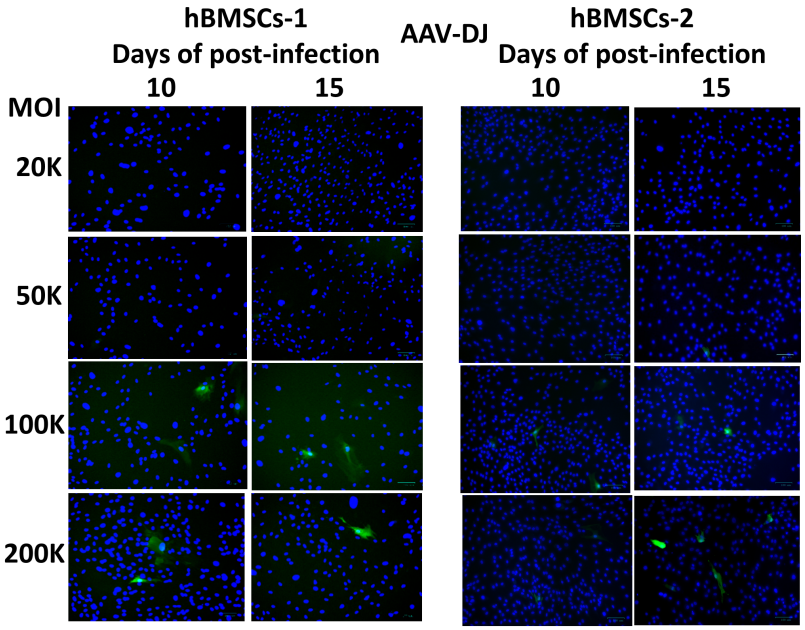

Fig. 3

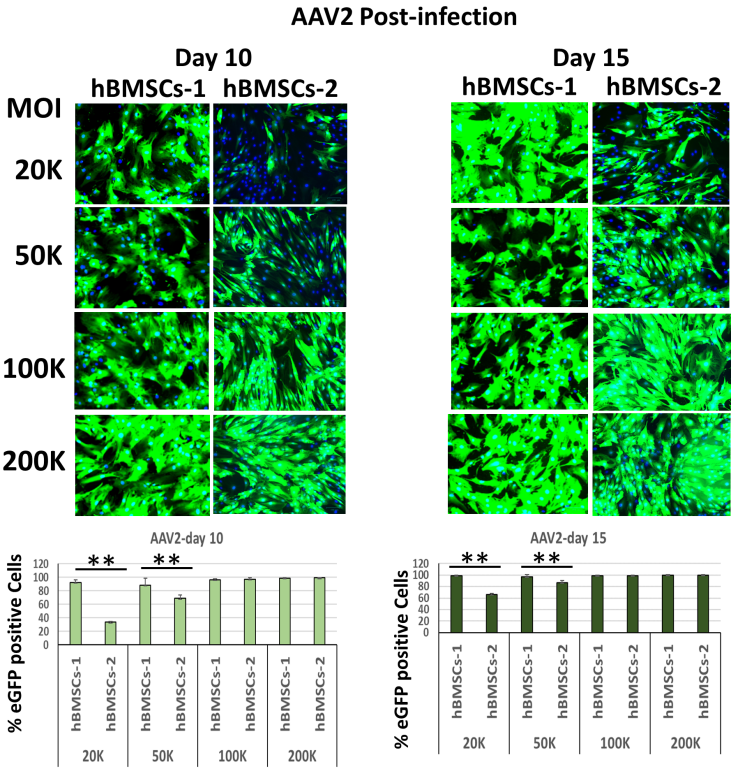

Fig. 4

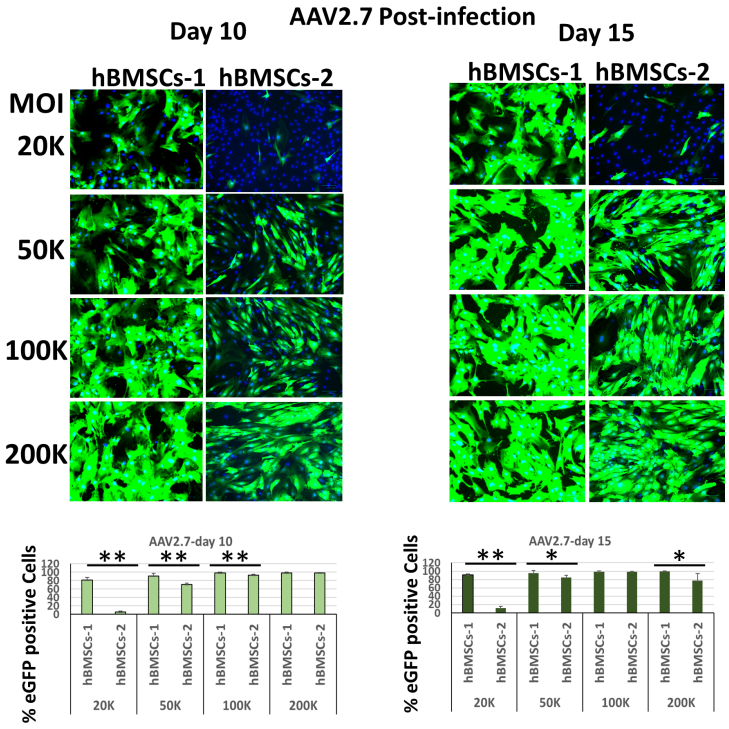

Fig. 5

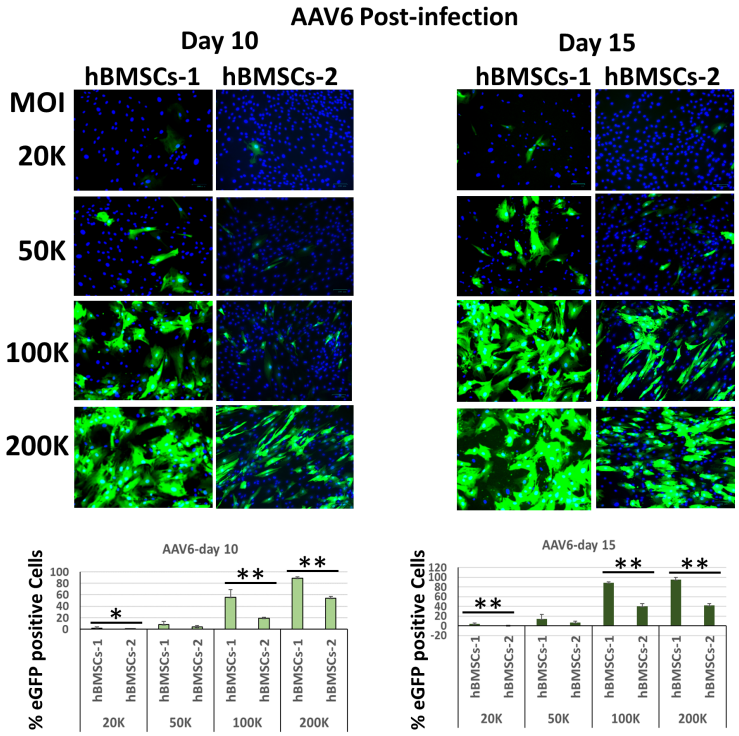

Fig. 6

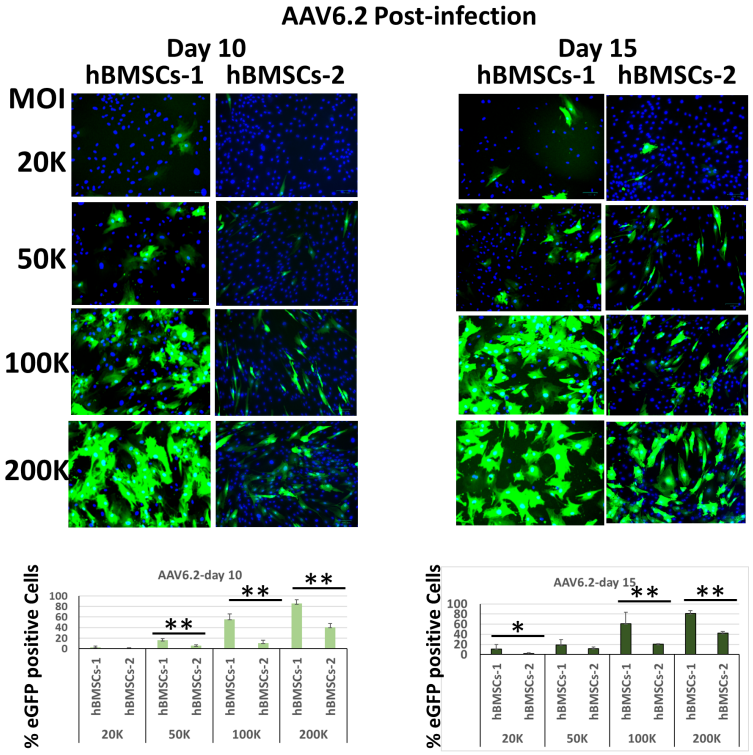

Fig. 7

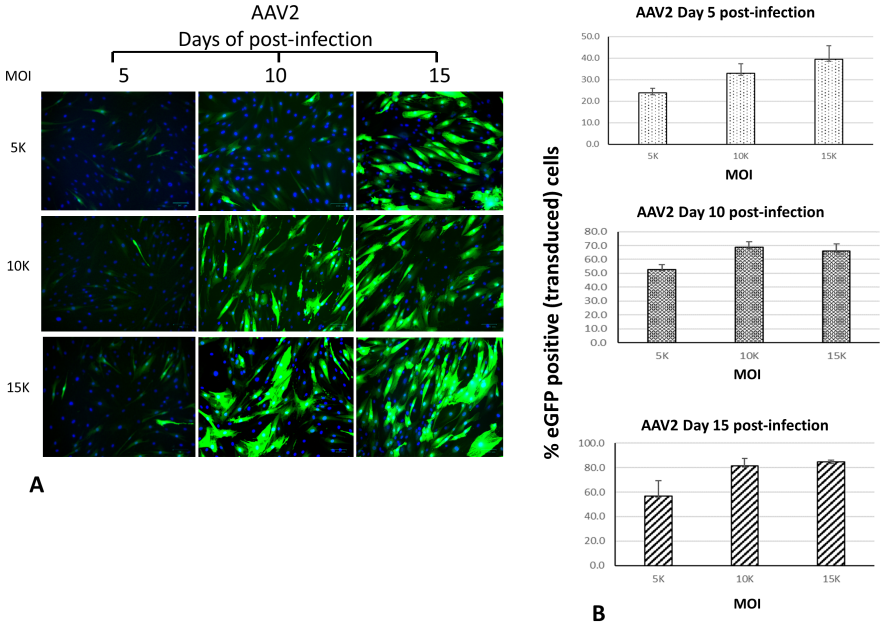

Fig. 8

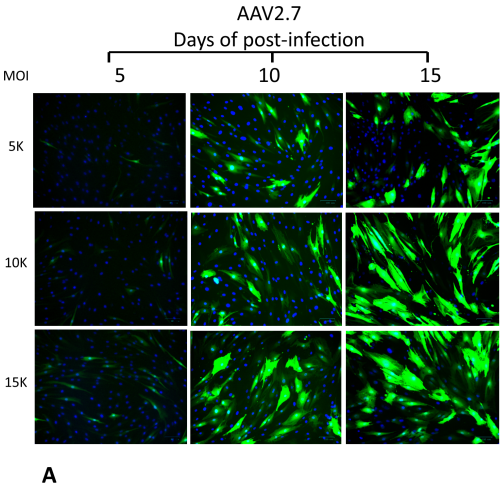

A

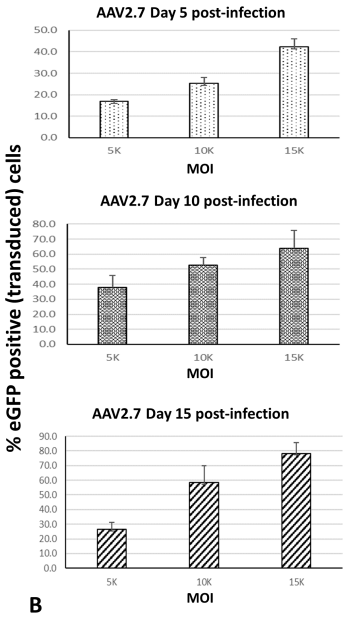

B

Fig. 9

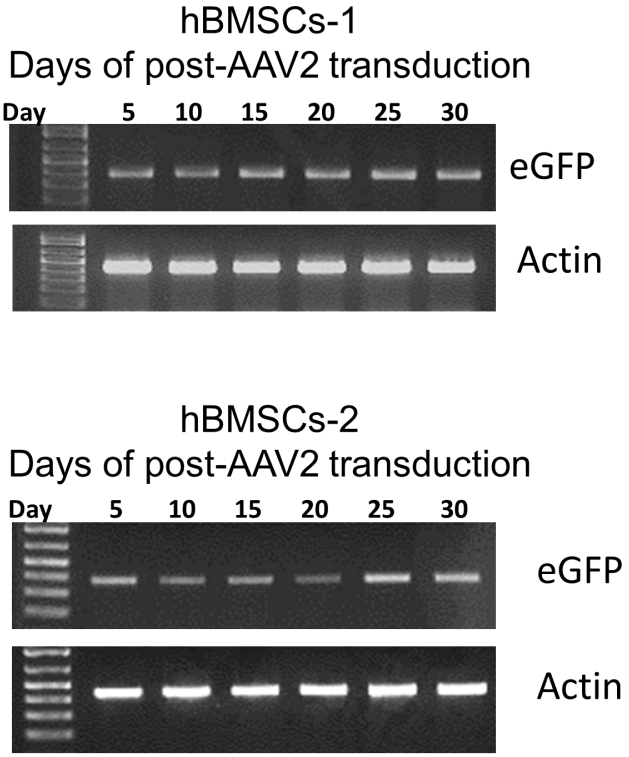

Fig. 10